Eur. Phys. J. D **6**, 303–309 (1999)

THE EUROPEAN PHYSICAL JOURNAL D

EDP Sciences

Doppler limited laser spectroscopy on hafnium lines. Part I: Hyperfine structure of even-parity levels

S. Bouazza[1,a], M. Fienhold[2], G.H. Guthöhrlein[2,b], H.O. Behrens[2], and J. Dembczynski[3]

[1] Département de Physique, Faculté des Sciences, B.P. 1039, 51687 Reims Cedex, France
[2] Universität der Bundeswehr Hamburg, Holstenhofweg 85, 22043 Hamburg, Germany
[3] Politechnika Poznanska, Katedra Fizyki Atomowej, ul. Piotrowo 3, 60-965 Poznan, Poland

Received: 28 October 1998 / Received in final form: 12 January 1999

Abstract. High-resolution Doppler limited hyperfine structure investigations done by laser spectroscopy techniques using laser induced fluorescence and optogalvanic detection are performed in the plasma of a liquid nitrogen cooled hollow cathode discharge in the atomic spectrum of Hafnium on selected lines in the red spectral region. Hyperfine structure spectra obtained using an enriched sample of ^{177}Hf yielded hyperfine structure constants A and B of both transition levels. For the first time, an experimentally derived description of the levels of the $5d^3 6s$ configuration are presented. Combined with previously obtained data, the hyperfine structure of altogether 12 fine structure levels has been analysed by the simultaneous parametrisation of the one- and two-body interactions in the atomic hyperfine structure for the model space $(5d + 6s)^4$.The radial parameters of the magnetic dipole and electric quadrupole interactions are determined for the configurations $5d^2 6s^2$, $5d^3 6s$ and $5d^4$ and compared with *ab initio* calculations. Finally a complete list of the predicted hyperfine structure constants A and B of all levels of the system was generated.

PACS. 31.30.Gs Hyperfine interactions and isotope effects, Jahn-Teller effect

1 Introduction

Most hyperfine structure (hfs) and isotope shift measurements have been performed on the $4d$- and $5d$-shell elements using Fabry-Perot interferometry and hollow cathode light sources [1–7]. However, more accurate measurements of the hfs have been limited to low-lying levels due to the high evaporation temperature of many of the refractory elements. Hafnium ($Z = 72$), together with titanium and zirconium, belongs to group IV of the transition metals in the periodic system. Its melting point is 2227 °C and its boiling point is 4602 °C. ^{177}Hf and ^{179}Hf are the only stable isotopes with the non-zero nuclear spins, of $I = 7/2$ and $I = 9/2$, respectively. Furthermore one can expect that the electric-quadrupole interaction brings, on the average, the major contribution to the level hfs since $\frac{Q_{5d}}{g_I}$ (^{177}Hf) is 15 times greater than $|\frac{Q_{3d}}{g_I}$ (^{47}Ti)|, where the hyperfine splittings are already sensitive to the quadrupole interaction unlike that for ^{141}Pr or ^{51}V for example.

The development of various methods for producing intense atomic beams [8–11] and the introduction of laser spectroscopic techniques have considerably improved the possibilities for performing hfs measurements on refractory elements [12]; however, when compared to other elements only a small number of hfs investigations have been performed on hafnium [13–18].

Previously, using configuration mixing and two-body hfs contributions [19] similar to those used for the tantalum atom [20], we have been able to predict the hfs of the levels of $5d^3 6s$ configuration of the hafnium atom based upon five experimental data found in the literature [13–18]. The aim of this present work is to obtain new experimental hfs data and to test the previously predicted hyperfine constants.

2 Procedures

2.1 Experimental

A schematic experimental set-up for laser induced fluorescence (LIF) and optogalvanic(OG) detection is shown in Figure 1. The detection is readily interchangeable and is achieved by merely pressing the switch in front of the lock-in amplifier. The intensity modulated laser beam passes axially through the bore of the hollow cathode lamp. For the LIF experiment, the fluorescent light was collected and directed to the entrance slit of the monochromator by mirrors and lenses. A hole was drilled into mirror M4 so that the laser beam could exit. This allows the uncoupling of the fluorescent light path from the laser light path.

[a] e-mail: safa.bouazza@univ-reims.fr
[b] e-mail: guenter.guthoehrlein@unibw-hamburg.de

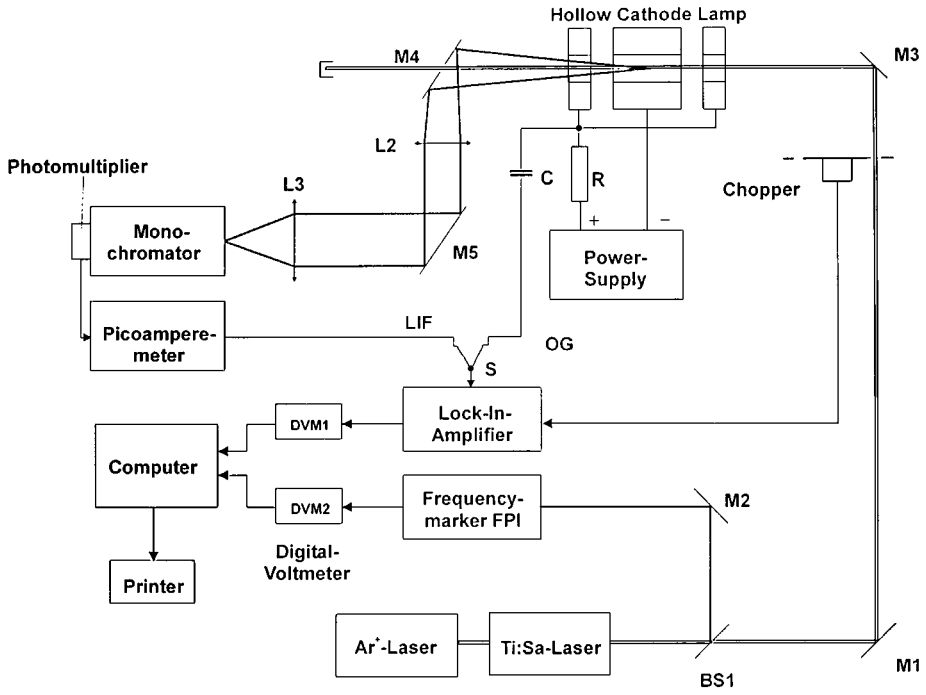

Fig. 1. Experimental set-up for laser induced fluorescence spectroscopy (LIF) and otogalvanic detection (OG).

A selected wavelength of fluorescence is filtered out by a McPherson 2061 grating monochromator with high dispersion. The light output of the monochromator is recorded by a photomultiplier (Hamamatsu R928). The ac component of the photocurrent is amplified and fed as input signal to a lock-in amplifier. The output of the lock-in, as well as the frequency marks for calibration of the linearity of the laser scan, are digitized by means of two digital voltage meters and transferred to a personal computer for storage and further data handling. Since the OG sensitivity was inferior to that of LIF for the majority of the spectral lines, we applied LIF detection in most cases to measure the hfs of a spectral line. For this purpose the transmission wavelength of the monochromator was fixed on a preselected fluorescence line, representing a decay from either of the two energy levels the laser combines, and the laser frequency was scanned (scanwidth: 25GHz) across the hfs. We chose a detection line for laser induced fluorescence which was different from the excitation line in order to avoid stray laser light. In most cases, the selected detection line had the additional advantage of possessing a higher transition probability.

An actively stabilized cw titan-sapphire laser (Coherent, model 899-21) pumped by an argonion laser (15 W) was used as laser source. Typical single mode output power was 1W in the red region (780–915 nm). The laser light was chopped in order to allow for lock-in amplification technique.

As a sputtering source we used a liquid nitrogen cooled, slightly modified, Schüler-type hollow cathode discharge [21] in order to produce a proper density of hafnium atoms. A 0.25 mm thick cylindrical metalic foil of hafnium (97.0% purity) in the natural isotope mixture was inserted into the bore of a copper cathode. For the measurements with the enriched ^{177}Hf isotope probe, 20 mg of enriched hafnium oxide powder was rubbed on the wall of the cylindrical bore of an aluminium cathode. The relative abundancies of the isotopes in the probe, as given by the supplier, were as follows: ^{174}Hf: 0.62%, ^{176}Hf: 0.87%, ^{177}Hf: 91.38%, ^{178}Hf: 4.92%, ^{179}Hf: 1.01%, and ^{180}Hf: 1.80%. The diameter of the bore of the cathodes was 3 mm. The two anodes having a bore of the same diameter were made of pure aluminium. Argon at a pressure of approximately 1 mbar was used as carrier gas. The typical discharge current was 40 mA.

The basis to the LIF experiment can be described as follows: when the laser frequency is tuned to the center frequency of a hyperfine component, those atoms which resonantly absorb the laser light are excited. The subsequent modulation in the population of either of the combining energy levels leads to a modulation of the fluorescence intensity, which marks those fluorescence lines that originate from either of the two involved levels of the excitation transition. Tuning the transmission wavelength of the monochromator across the spectrum permits the selection of modulated lines. Phase sensitive detection with a lock-in amplifier then allows the detection of these lines, discriminating between modulated and non-modulated lines. Furthermore the phase sensitive detection lock-in differentiates between fluorescence lines originating from the

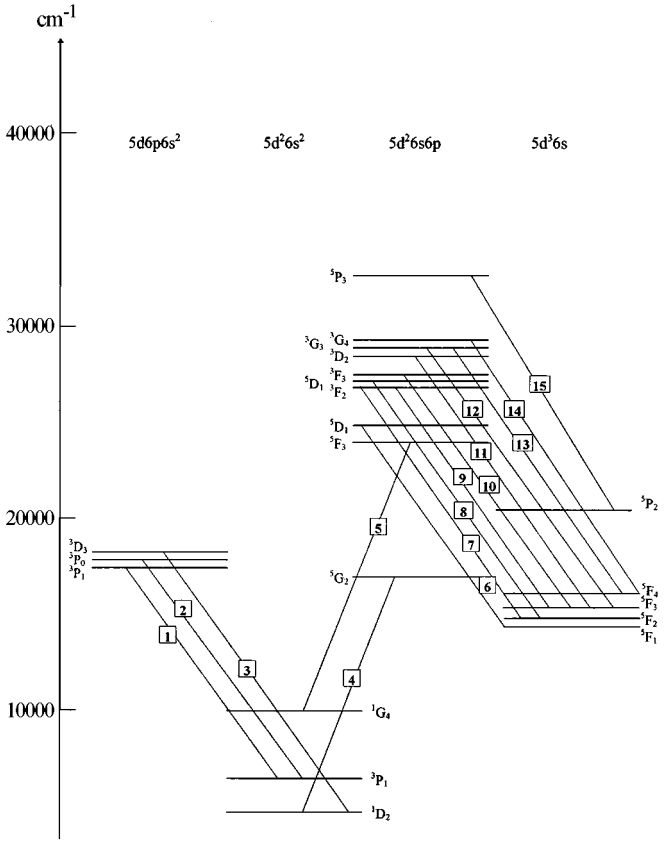

Fig. 2. Investigated lines in this work (see Tab. 1).

upper and lower transition levels according to the phase of the modulation of the fluorescence lines.

The intensity of a fluorescence line is proportional to the population of the level. Thus, as laser induced absorption enhances the population of the upper level in phase with the modulation frequency of the laser beam, the fluorescence lines originating from the upper level are in phase. Laser induced absorption at the same time diminishes the population of the lower level of the transition and thus the corresponding fluorescence lines originating from the lower transition level antiphase modulated (180°) out of phase) compared with the intensity modulation phase of the laser beam.

Figure 2 shows part of the level diagram of Hf I and the lines that we studied and Figure 3 shows an example of the hyperfine spectrum of the ^{177}Hf line $\lambda = 8080.265$ Å.

Table 1 lists the studied spectral lines with classification and Table 2 gives the experimental hfs data of three levels of the $5d^26s^2$ configuration and five of the $5d^36s$ one.

2.2 Semi-empirical determination of the hfs radial parameters

The method applied here for fine structure (fs) analysis [22], has been successfully used to study cobalt [23], titanium [24–26], zirconium [27], hafnium [19], and tantalum [20] atoms. In our previous work [19] we presented

Table 1. List of studied lines, all located in red region. T_i is the energy value of the lower even-level belonging to configurations: $5d^26s^2$ or $5d^36s$; T_u is the energy value of the upper old level belonging to configurations: $5d6p6s^2$ or $5d^26s6p$. N is referred to as line number in Figure 2.

λ_{air} (nm)	lower level	T_i (cm^{-1})	upper level	T_u (cm^{-1})	N
864.004	a ^{3}P$_1$	6573	z ^{3}P$_1$	18143	1
854.643	a ^{3}P$_1$	6573	z ^{3}P$_0$	18270	2
784.537	a ^{1}D$_2$	5639	z ^{3}D$_3$	18382	3
808.026	a ^{1}D$_2$	5639	z ^{5}G$_2$	18011	4
774.017	a ^{1}G$_4$	10533	z ^{5}F$_3$	23448	5
900.474	a ^{5}F$_1$	14092	z ^{5}D$_1$	25194	6
805.647	a ^{5}F$_2$	14741	y ^{3}F$_2$	27150	7
781.457	a ^{5}F$_2$	14741	y ^{5}D$_1$	27533	8
871.120	a ^{5}F$_3$	15673	y ^{3}F$_2$	27150	9
834.425	a ^{5}F$_3$	15673	y ^{3}F$_3$	27654	10
793.806	a ^{5}F$_3$	15673	y ^{3}D$_2$	28267	11
774.357	a ^{5}F$_3$	15673	z ^{3}G$_3$	28584	12
846.000	a ^{5}F$_4$	16767	z ^{3}G$_3$	28584	13
801.058	a ^{5}F$_4$	16767	z ^{3}G$_4$	29247	14
817.390	a ^{5}P$_2$	20908	z ^{5}P$_3$	33139	15

Table 2. The hyperfine structure constants A and B determined from laser induced fluorescence measurements.

Level		Energy (cm^{-1})	$A_{\rm exp}$ (MHz)	$B_{\rm exp}$ (MHz)
$5d^26s^2$	^{3}P$_1$	6572.54	21.4 ± 0.8	758 ± 12
	^{1}D$_2$	5638.61	75.2 ± 0.3	-815 ± 13
	^{1}G$_4$	10532.55	75.1 ± 0.6	4264 ± 9
$5d^36s$	^{5}F$_1$	14092.26	-506.2 ± 0.8	-326 ± 7
	^{5}F$_2$	14740.67	160.0 ± 0.2	-338 ± 2
	^{5}F$_3$	15673.32	272.4 ± 0.4	-518 ± 2
	^{5}F$_4$	16766.60	298.1 ± 0.2	-745 ± 12
	^{5}P$_2$	20908.43	614.0 ± 3.0	-1478 ± 19

the radial parameters obtained from the fs least squares fit (FS LSF) to the experimental energy levels [28]. These values have been used for the calculation of the intermediate wave functions and for assumptions needed for hfs parametrisation performed in this work, seeing the large number of one- and two-body hfs parameters [22] and the smaller number of hafnium hfs experimental data. The theory assumes that the electron excitation $nd \rightarrow n''d$ affects the spin-orbit splitting, the magnetic-dipole and the electric-quadrupole hyperfine structure in the same way, as has been confirmed in some cases for the $3d$-atoms [23, 24] and used previously for $5d$-element like tantalum [20]. We have assumed therefore that the ratios between two-body hfs parameters a_i or b_i $(i = 1, 2, 3)$ and one-body hfs parameters a^{01}_{5d} or b^{02}_{5d} remain the same as between the two-body spin-orbit parameters P_i and one-body spin-orbit

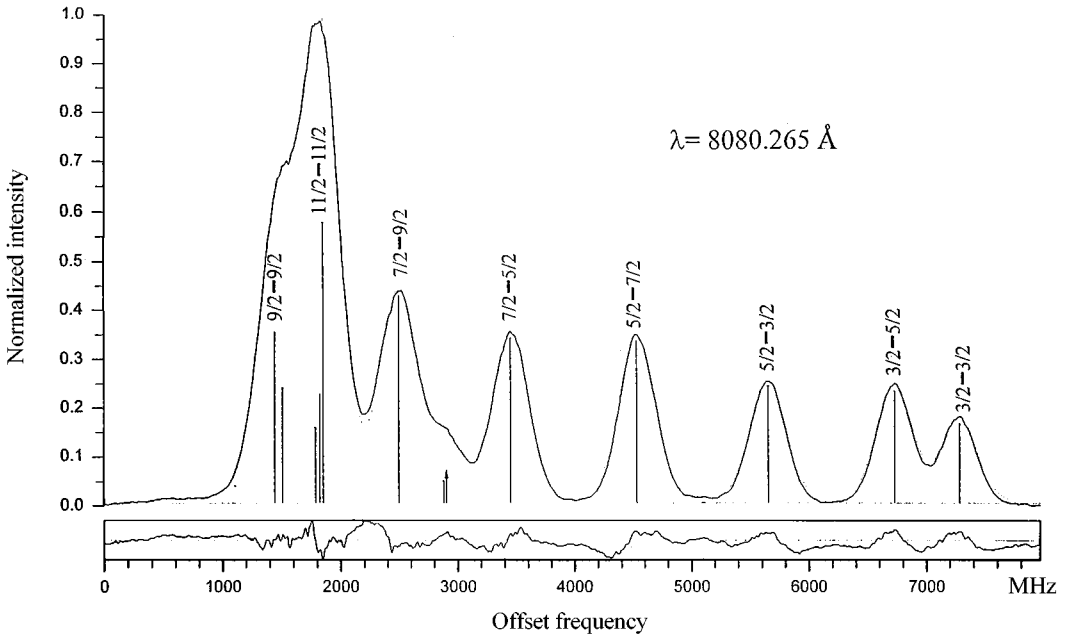

Fig. 3. Experimental and computed profiles of the $\lambda = 808.0265$ nm line and below the difference between them. For the strongest or well-isolated hyperfine components the F quantum numbers of upper and lower hyperfine levels are inserted.

ones ζ [23], obtained from the fs fit as the following:

$$a^{01}_{5d} : a_1 : a_2 : a_3 = \zeta(5d, 5d) : P_1 : P_2 : P_3\,,$$

and

$$b^{02}_{5d} : b_1 : b_2 : b_3 = \zeta(5d, 5d) : P_1 : P_2 : P_3\,.$$

It is important to note that since the tensorial ranks κk differ, the correspondence between the 3 two-body spin-orbit parameters and the two-body hfs parameters is $\frac{a_i}{a^{\kappa k}_{5d}} = \frac{b_i}{b^{\kappa k}_{5d}} = \frac{P_i}{\zeta(5d5d)}$. This allows the possibility to compare the effects of the virtual excitations on the fine and hyperfine structure, or to introduce in hfs-fit fixed relations between radial parameters. The other principles of the model space method are described, for instance, in [27].

Table 3 contains the values of fitted hfs parameters and other assumed constraints obtained from the fs fit. As in our previous work [19], we used Hartree-Fock calculations to deduce the assumption necessary for fitting of the experimental data. In addition we were obliged to assume that the ratio between a_9 and a^{10}_{6s} is the same as that of tantalum [20] (on the other hand, we let a_{11} free).

For the hafnium atom, theoretical calculations are not available for the model space parameters at this time; usually the hfs parameters are discussed separately for each configuration. Using previously established relationships, given in [22], the corresponding parameters for each configuration have been deduced from the model space parameters. For the lowest even configurations they are gathered in Table 4, together with values gleaned from the literature which only exist for the $5d^26s^2$ configuration [14, 15,18]. For determination of the one-electron radial integrals, we used the electric quadrupole moment, free of Sternheimer shielding effect [29,30], $Q_{5d} = 3.365$ (29) b of ^{177}Hf which has been determined using muonic M X-rays, by Tanaka *et al.* [31], and the nuclear factor $g_I = 0.2267$ (2), given by Raghavam [32].

The configuration radial integrals are given in Table 5 together with the results of relativistic Hartree-Fock calculations performed by Olsson and Rosén [33].

For the first time, the values of the $\langle r^{-3}\rangle^{\kappa k}_{5d}$ and $\langle r^{-3}\rangle^{10}_{6s}$ for the $5d^36s$ configuration have been determined within the model space $(5d + 6s)^4$. Rather like the tantalum atom [20], the derived value of $\langle r^{-3}\rangle^{10}_{6s}$ is close to the theoretical one obtained from Hartree-Fock calculations.

The experimental value $\langle r^{-3}\rangle^{10}_{5d}$ reflects relativistic effects and the core polarisation contribution due to the Fermi contact term [34]: $\langle r^{-3}\rangle^{10}_{5d,\mathrm{exp}} = \langle r^{-3}\rangle^{10}_{5d,\mathrm{rel}} + \langle r^{-3}\rangle^{10}_{5d,\mathrm{contact}}$.

As can be seen from *ab initio* theoretical calculations [33] given in Table 5, the relativistic parts are negative and differ significantly from the observed ones.

It should be pointed out that the core polarisation contribution for $5d^26s^2$ configuration is positive unlike that for the $3d^n4s^2$ configurations [23,24] and that the core polarisation contribution for the $5d^36s$ configuration is negative rather like that for the $3d^{n+1}4s$ configurations [23, 24]. This means that the contributions from the virtual excitations, *last full ns-shell→empty shell* are positive and overcompensate contributions from the excitations *inner full ns-shells→empty-shells.*

In Table 6 we present predicted A and B hyperfine constants of all known levels of the configurations $5d^26s^2$, $5d^36s$ and $5d^4$ for which hfs splittings have not yet been measured, expressed with relative uncertainties of 5% and 15%, respectively.

Table 3. The hfs many-body parameters for the model space $(5s+6s)^4$ of the ^{177}HF (in MHz). The uncertainties given in parentheses are the standard deviations.

a^{01}_{5d}		87.13 (0.50)	b^{02}_{5d}		4890 (14)
a^{12}_{5d}	$= 1.233\, a^{01}_{5d} =$	107.44[a]	b^{13}_{5d}		1646 (122)
a^{10}_{5d}		58.00 (2.95)	b^{11}_{5d}		−323 (56)
a^{10}_{6s}		2452 (11)			
a^{12}_{IC}		37 (10)	b^{02}_{IC}		980 (67)
a_1	$= 0.2318\, a^{01}_{5d} =$	20.20[b]	b_1	$= 0.2318\, b^{02}_{5d} =$	1133[b]
a_2	$= 0.0298\, a^{01}_{5d} =$	2.60[b]	b_2	$= 0.0298\, b^{02}_{5d} =$	146[b]
a_3	$= 0.0200\, a^{01}_{5d} =$	1.74[b]	b_3	$= 0.0200\, b^{02}_{5d} =$	98[b]
a_9	$= 0.179\ \ a^{10}_{6s} =$	439[c]			
a_{11}		−1369 (39)			

[a] Ratio of the parameters taken from relativistic Hartree-Fock calculation [33].
[b] Ratio of the parameters taken from FS LSF (see text).
[c] Ratio of the parameters taken from hfs fit for Ta [20].

Table 4. The experimental one-electron radial parameters of the three configurations of the model space $(5d+6s)^4$ given in MHz.

Config.	a^{01}_{5d}	a^{12}_{5d}	a^{10}_{5d}	a^{10}_{6s}	b^{02}_{5d}	b^{13}_{5d}	b^{11}_{5d}	Ref.
$5d^26s^2$	85.705	23.245	15.760		4662.694	2324.645	882.206	[14,18]
	79.05	99.36	58.00		4436.7	1646.1	−323	this work
$5d^36s$	70.97	91.28	−117.6	2452	3983.5	1646.1	−323	this work
$5d^{4(*)}$	62.89	83.20	−117.6		3530.3	1646.1	−323	this work

(*) Derived from the parameters of the $5d^26s^2$ or $5d^36s$ configurations (given above) using relations (12) of [24].

Table 5. The experimental hfs radial integrals and corresponding theoretical values of the three configurations of the model space $(5d+6s)^4$ given in atomic units. HF: relativistic Hartree-Fock method [33].

Config.	$\langle r^{-3}\rangle^{01}_{5d}$	$\langle r^{-3}\rangle^{12}_{5d}$	$\langle r^{-3}\rangle^{10}_{5d}$	$\langle r^{-3}\rangle^{10}_{6s}$	$\langle r^{-3}\rangle^{02}_{5d}$	$\langle r^{-3}\rangle^{13}_{5d}$	$\langle r^{-3}\rangle^{11}_{5d}$	Ref.
$5d^26s^2$	3.65	4.59	2.68		5.61	2.08	−0.40	this work
	4.02	1.09	0.74					[14]
	4.09	0.46	−0.134					[36]
	4.21	5.19	$-0.43^{(*)}$		4.33	2.36	−0.78	HF
$5d^36s$	3.28	4.22	−5.44	170.04	5.04	2.08	−0.40	this work
	3.64	4.58	$-0.42^{(*)}$	181.4	3.74	2.17	−0.74	HF
$5d^{4(**)}$	2.91	3.85	−5.44		4.47	2.08	−0.40	this work
	3.17	4.09	$-0.42^{(*)}$		3.25	2.03	−0.73	HF

(*) Relativistic part only (the contributions of spin polarisation have not been taken into account).
(**) See remark given in Table 4.

3 Conclusion

This work has demonstrated that hafnium is an excellent candidate for studying two-body hfs effects. Using the values of Table 6, one can check in most cases that the ratio between the hfs factors B and A is greater than the inverse ratio of their respective coefficients in the well-known Casimir formula. This verification confirms that the electric-quadrupole interaction has a dominating contribution in hyperfine splitting as a whole.

Very good experimental accuracy can be achieved for the B-constants of the high-lying levels. Therefore the increasing body of experimental data coupled to the improvement of intermediate coupling wave functions should permit the determination of all one- and two-body contributions [22]—which are in fact another form of Sternheimer corrections—to the B-constants. Having achieved this it will be possible to compare the Q-values obtained from muonic M X-rays and from optical spectra. A first look at Table 5, which reveals a real agreement between experimental and theoretical values of $\langle r^{-3}\rangle^{13}_{5d}$, may confirm our above conclusions. It is noteworthy that electrostatic interactions with distant configurations do not provide any contributions with respect to the $\kappa k = 13$ and $\kappa k = 11$ [35]. Hence one can consider that the hfs radial parameters b^{13} and b^{11}, correctly determined, *i.e.* devoid

Table 6. Predicted A and B hfs constants of ^{177}Hf (in MHz). The rows printed in bold are related to the levels with experimental measured hfs splitting.

Energy			Designation	$A_{\rm exp}$	$A_{\rm calc}$	ΔA	$B_{\rm exp}$	$B_{\rm calc}$	ΔB
J = 1									
6572.54	***f***	I	**^{3}P**	**21.4**	**23.1**	**−1.7**	**758**	**739.5**	**18.5**
14092.26	***f***	II	**^{4}F; ^{5}F**	**−506.0**	**−518.6**	**12.6**	**−326**	**− 357.3**	**31.3**
20784.87	*f*	II	^{4}P; ^{5}P		858.4			193.3	
23641.35	*f*	II	^{2}D; ^{3}D		−437.3			− 922.6	
26918.13	*f*	II	^{2}P; ^{3}P		924.5			669.4	
28527.98	*f*	II	^{4}P; ^{3}P		−95.6			− 605.0	
32091.60	*f*	II	^{2}P; ^{1}P		−435.7			− 419.9	
37305*		II	^{2}D; ^{3}D		−536.0			979.7	
40618.63		III	^{5}D		−59.9			615.6	
J = 2									
0.000	***f***	I	**^{3}F**	**113.433**	**116.10**	**−2.667**	**624.33**	**595.2**	**29.13**
5638.61	***f***	I	**^{1}D**	**75.2**	**73.1**	**2.1**	**−815**	**− 862.8**	**47.8**
8983.74	***f***	I	**^{3}P**	**70.51**	**68.5**	**2.01**	**−1208.50**	**− 1203.3**	**− 5.2**
14740.67	***f***	II	**^{4}F; ^{5}F**	**160.0**	**152.2**	**7.8**	**−338**	**− 361.6**	**23.6**
20908.43	***f***	II	**^{4}P; ^{5}P**	**614.0**	**604.3**	**9.7**	**−1478**	**−1533.2**	**55.2**
23327.71	*f*	II	^{4}F; ^{3}F		346.1			−1204.7	
25084.16	*f*	II	^{2}D; ^{3}D		422.5			−1359.3	
28200.54	*f*	II	^{2}P; ^{3}P		322.3			− 14.3	
30146.40	*f*	II	^{4}P; ^{3}P		−171.6			1272.6	
31119.20	*f*	II	^{2}F; ^{3}F		−256.6			474.6	
31619.97	*f*	II	^{2}D; ^{1}D		−88.1			272.4	
37282*		II	^{2}D; ^{3}D		290.3			686.4	
40260*		II	^{2}D; ^{1}D		79.5			2139.8	
40260*		II	^{2}D; ^{1}D		79.5			2139.8	
41211.02		III	^{5}D		−41.9			491.0	
J = 3									
2356.68	***f***	I	**^{3}F**	**80.7066**	**79.75**	**0.9566**	**823.950**	**802.1**	**21.85**
15673.32	***f***	II	**^{4}F; ^{5}F**	**272.4**	**266.1**	**6.3**	**−518.1**	**− 513.8**	**−4.3**
22199.08	*f*	II	^{4}P; ^{5}P		442.1			1505.3	
22880.24	*f*	II	^{2}G; ^{3}G		−199.3			954.4	
25281.82	*f*	II	^{4}F; ^{3}F		107.0			− 953.3	
26715.38	*f*	II	^{2}D; ^{3}D		312.5			− 921.0	
31054.64	*f*	II	^{2}F; ^{3}F		184.6			1583.9	
34274.21	*f*	II	^{2}F; ^{1}F		65.1			1563.4	
37257*		II	^{2}D; ^{3}D		477.0			1758.1	
41739.39		III	^{5}D		−25.1			− 381.7	
J = 4									
4567.64	***f***	I	**^{3}F**	**69.04**	**71.8**	**−2.76**	**1432.77**	**1338.5**	**94.27**
10532.55	***f***	I	**^{1}G**	**75.1**	**75.5**	**−3.6**	**4264**	**4277.5**	**−13.5**
16766.60	***f***	II	**^{4}F; ^{5}F**	**298.1**	**295.6**	**2.5**	**−745**	**− 725.1**	**−19.9**
23252.81	*f*	II	^{2}G; ^{3}G		89.4			1557.3	
25678.61	*f*	II	^{2}H; ^{3}H		−2.5			1946.7	
27074.50	*f*	II	^{4}F; ^{3}F		−118.3			− 410.1	
30501.08	*f*	II	^{2}G; ^{1}G		44.7			744.6	
31575.68	*f*	II	^{2}F; ^{3}F		260.3			1033.7	
42175.62	*f*	III	^{5}D		−10.7			−2027.7	
J = 5									
17901.28	*f*	II	^{4}F; ^{5}F		309.2			971.6	
24085.14	*f*	II	^{2}G; ^{3}G		311.0			− 781.5	
27018.75	*f*	II	^{2}H; ^{3}H		156.0			− 687.9	
31764*		II	^{2}H; ^{1}H		41.0			− 582.9	
J = 6									
26943.95	*f*	II	^{2}H; ^{3}H		286.8			− 729.4	

* Predicted energy values; I: $5d^26s^2$; II: $5d^36s$; III: $5d^4$; f: level energy included in the fine structure least squares fit.

of uncertainties arising from eigenvector compositions and without any additional assumptions being introduced during the hfs parametrisation procedure, are free from Sternheimer corrections.

Moreover we intended to test our predictions and our experimental hfs data confirmed the well-founded basis of our approach. In our fine structure study we had recurred to only three interacting configurations. Therefore a considerable amount of work remains to be carried out in order to provide a more complete description of all of the possible interacting configurations. Presently work is under way which should allow us to advance towards this goal. Indeed, we intend to consider a set of configurations which intimately interact with each other because some perturbation resonances surely exist between the levels of the $(5d + 6s)^4$ configurations and configurations containing paired $6p$-electrons which involve some deviations with regard to the hfs of the levels of different configurations which are close to each other.

We invite our colleagues to join us in solving this exciting but laborious problem.

References

1. H. Kopfermann, *Nuclear Moments*, editedy by E.E. Schneider (Academic Press, New York, 1958).
2. N.F. Ramsey, *Molecular Beams* (Oxford University Press, London, 1956).
3. A.J. Freeman, R.B. Frankel (Editors), *Hyperfine Interaction* (Academic Press, New York, 1967).
4. G. Breit, Phys. Rev. **35**, 1447 (1930).
5. G. Racah, Nuovo Cimento **8**, 178 (1931).
6. W.J. Childs, Case Studies Atomic Phys. **3**, 215 (1973).
7. S. Bouazza, J. Bauche, Z. Phys. D **10**, 1 (1988).
8. W.M. Doyle, R. Marrus, Nucl. Phys. **49**, 449 (1963).
9. S. Büttgenbach, G. Meisel, S. Penselin, K.H. Schneider, Z. Phys. **230**, 329 (1970).
10. J.M. Pendlebury, D.B. Ring, J. Phys. B **5**, 386 (1972).
11. H. Rubinsztein, I. Lindgren, L. Lindstrom, H. Riedl, A. Rosén, Nuclear Instr. Methods **119**, 269 (1974).
12. W. Ertmer, B. Hofer, Z. Phys. A **276**, 9 (1976).
13. D. Zimmermann, P. Baumann, D. Kuszner, D. Werner, Phys. Rev. A **50**, 1112 (1994).
14. S. Büttgenbach, R. Dicke, H. Gebauer, Phys. Lett. A **62**, 307 (1977).
15. S. Büttgenbach, M. Herschel, G. Meisel, E. Schrodl, W. White, Z. Phys. **260**, 157 (1973).
16. A. Anastassov, Yu.P. Gangrsky, B.K. Kul'djanov, K.P. Marinova, B.N. Markov, S.G. Zemlyanoi, Z. Phys. A **348**, 177 (1994).
17. A. Anastassov, Yu.P. Gangrsky, K.P. Marinova, B.N. Markov, B.K. Kul'djanov, S.G. Zemlyanoi, Hyperfine Inter. **74**, 31 (1992).
18. W.J. Jin, M. Wakasugi, T.T. Inamura, T. Murayama, T. Wakui, H. Katsuragawa, T. Ariga, T. Ishizuka, I. Sugai, Phys. Rev. A **52**, 157 (1995).
19. J Dembczynski, S. Bouazza, G. Szawiola, J. Ruczkowski, J. Phys. II **7**, 1175 (1997).
20. J. Dembczynski, B. Arcimowicz, G.H. Guthöhrlein, L. Windholz, Z. Phys. D **39**, 143 (1997).
21. H. Schüler, Z. Phys. **59**, 149 (1930).
22. J. Dembczynski, W. Ertmer, Y. Johann, P. Unkel, Z. Phys. A **321**, 1 (1985).
23. J. Dembczynski, G.H. Guthöhrlein, E. Stachowska, Phys. Rev. A **48**, 2752 (1993).
24. R. Aydin, E. Stachowska, U. Johann, J. Dembczynski, P. Unkel, W. Ertmer, Z. Phys. D **15**, 281 (1990).
25. E. Stachowska, M. Fabiszisky, M. Christ, A. Scholz, U. Sterr, W. Ertmer, Z. Phys. D **27**, 303 (1993).
26. E. Stachowska, M. Fabiszisky, J. Dembczynski, Z. Phys. D **32**, 27 (1994).
27. S. Bouazza, J. Dembczynski, E. Stachowska, G. Szawiola, J. Ruszkowski, Eur. Phys. J. D **4**, 39 (1998).
28. W.F. Meggers, C.E. Moore, N.B.S. Monograph **153** (1976).
29. R.M. Sternheimer, R.F. Peierls, Phys. Rev. A **3**, 387 (1971).
30. R.M. Sternheimer, Phys. Rev. A **146**, 140 (1996).
31. Y. Tanaka, R.M. Steffen, E.B. Shera, W. Reuter, M.V. Hoehn, J.D., Zubro, Phys. Rev. C **29**, 1830 (1984).
32. P. Raghavam, At. Data Nucl. Data Tables **42**, 189 (1989).
33. G. Olsson, A. Rosén, Phys. Scripta **26**, 168 (1982).
34. B.R. Judd, Proc. Phys. Soc. **82**, 874 (1963).
35. L. Armstrong Jr., *Theory of the Hyperfine Structure of Free Atoms* (Wiley Interscience, New York, 1971).
36. S. Büttgenbach *Hyperfine Structure in 4d- and 5d-Shell Atoms*, Springer Tracts Mod. Phys. **96** (Springer Berlin, 1982).